Normal Mode Initialization Procedure Applied to Forecasts with the Global Shallow Water Equations

DAVID L. WILLIAMSON

National Center for Atmospheric Research,[1] Boulder, Colo. 80303

(Manuscript received 15 August 1975, in revised form 4 November 1975)

ABSTRACT

Conventional procedures designed to balance global initial data for primitive equation forecast models often result in unrealistic large-amplitude, high-frequency oscillations during the initial stages of the forecasts. In an attempt to reduce these oscillations, Dickinson and Williamson (1972) proposed a method to initialize data by expanding the data into the normal modes or free oscillations of the linearized version of the forecast model. Once the data are expanded into the normal modes, the modal amplitudes thought to be erroneously large can be reduced or set to zero. This procedure is tested here with the shallow water equations. In the first set of one-day forecasts performed, the method eliminates the large-amplitude, high-frequency waves which occur when using analyzed heights and winds for initial data by removing the gravity waves and computational Rossby waves from the initial data. The standard deviation of the error and the S_1 skill score show substantial improvement in the filtered case. This improvement is a result of the smoothing due to the initial filtering rather than an improvement in the forecast of the waves retained. When included, the gravity waves do not interact significantly with the Rossby waves during the one-day forecast.

Additional experiments are performed to examine the effect on the one-day forecast of removing the small-scale Rossby waves from the initial data. In general, except for the smallest longitudinal-scale Rossby waves, removal of these modes degrades the forecasts. A third set of forecasts examines the effect of the large-scale gravity waves on the forecast. The largest latitudinal-scale gravity waves have little effect on the forecast skill scores; they neither improve nor degrade the forecast with the shallow water equations. Inclusion of the medium- and smaller-scale gravity waves in the initial data degrades the forecasts. Several forecasts are repeated with the mean depth decreased. The conclusions with respect to the modal filtering are unchanged although the impact of the filtering is less dramatic in these cases. The results are also insensitive to the particular longitudinal filtering used near the poles to allow longer time steps.

1. Introduction

In recent years, the domain of numerical weather prediction models has been extended to include the entire globe. This has led to some difficulties in providing consistent heights and winds for initial data with primitive equation models. Conventional balancing procedures relating the winds and heights have been derived largely from analysis of motions on mid-latitude tangent planes (Hinkelmann, 1951; Charney, 1955), where there is a clear distinction between the gravity wave modes with relatively large divergence and the meteorologically more important quasi-geostrophic Rossby modes with divergence an order of magnitude smaller than vorticity (Phillips, 1963). These balancing procedures have been extended to the spherical rotating earth (Houghton and Washington, 1969) by assuming that pressure determines the wind in middle latitudes and that the wind field determines the pressure field in the tropics. The divergent component of the wind consistent with this balancing can also be obtained over the sphere (Houghton *et al.*, 1971). However, the methods proposed in these two papers apparently resulted in unrealistic oscillations during the initial stages of the integration with the NCAR general circulation model (GCM). Similar large oscillations have also been noted in integrations with a barotropic primitive equations model in spectral form (Rasmussen, 1974) from initial data satisfying the linear balance equation and with a baroclinic model in spectral form (Bourke, 1974) from initial nondivergent winds.

Washington and Baumhefner (1975) tested a method to reduce these unrealistic oscillations by setting the vertical mean mass divergence to zero at each grid point. In their example, the procedure reduces the amplitude of the Lamb waves by a factor of 3 and does not degrade the forecast accuracy. Their method is imposed only on the observed momentum field with no modification of the pressure field, and thus does not consider any relationship between the mass and mo-

[1] The National Center for Atmospheric Research is sponsored by the National Science Foundation.

mentum fields. Bourke (1974) added a divergence dissipation to his model and found it effective in eliminating spurious large-scale inertia-gravity oscillations during the course of the integration. As in the method of Washington and Baumhefner (1975), Bourke's method does not address inconsistencies in the initial mass and momentum fields.

Dickinson and Williamson (1972) proposed a method to initialize data for a particular model by expanding the data into the free oscillations or normal modes of the particular forecast model. Some of these model normal modes can be associated with the corresponding modes of the atmosphere and classified accordingly as Rossby or gravity modes. With the NCAR model, other modes are purely computational, arising from the particular numerical approximations used with the non-staggered grid of the model. Expansion of data into these modes allows selective identification and filtering of unwanted modes in the data. Thus after filtering, the mass and momentum fields are consistent with each other and with the forecast model within the context of the normal modes. In the following, this method provides filtered data for global forecasts with the shallow water equations.

2. Forecast model and initialization method

The forecast model consists of the discrete shallow water equations over a spherical grid defined by intersections of lines of constant latitude and longitude. Let $\Delta\varphi$ be the latitudinal grid increment, $\Delta\lambda$ the longitudinal grid increment, and Δt the temporal increment. We denote the value of some variable ψ at a grid point by

$$\psi^{\tau}_{i,j}=\psi[(i-1)\Delta\lambda,\quad (j-1)\Delta\varphi,\quad \tau\Delta t]=\psi(\lambda,\varphi,t). \tag{1}$$

We make use of the finite-difference operators

$$\left.\begin{aligned}\delta_\lambda\psi&=\frac{\psi^{\tau}_{i+1,j}-\psi^{\tau}_{i-1,j}}{2\Delta\lambda}\\ \delta_\varphi\psi&=\frac{\psi^{\tau}_{i,j+1}-\psi^{\tau}_{i,j-1}}{2\Delta\varphi}\\ \delta_t\psi&=\frac{\psi^{\tau+1}_{i,j}-\psi^{\tau-1}_{i,j}}{2\Delta t}\end{aligned}\right\}. \tag{2}$$

The discrete nonlinear shallow water equations of the model can then be written

$$\left.\begin{aligned}\delta_t u&=-\frac{u}{a\cos\varphi}\delta_\lambda u-\frac{v}{a}\delta_\varphi u+\left(f+\frac{u}{a}\tan\varphi\right)v-\frac{g}{a\cos\varphi}\delta_\lambda h\\ \delta_t v&=-\frac{u}{a\cos\varphi}\delta_\lambda v-\frac{v}{a}\delta_\varphi v-\left(f+\frac{u}{a}\tan\varphi\right)u-\frac{g}{a}\delta_\varphi h\\ \delta_t h&=-\frac{1}{a\cos\varphi}[\delta_\lambda(hu)+\delta_\varphi(hv\cos\varphi)]\end{aligned}\right\}, \tag{3}$$

where u, v and h are the grid point values of the zonal wind, meridional wind and height, g is gravity, a the radius of the earth, and f the Coriolis parameter. To save space, the approximations used at the poles are not included here. Those used at the North Pole are given by Eqs. (3.16)–(3.18) in Williamson and Browning (1973). The same approach is used to derive the corresponding approximations at the South Pole.

The linearized version of the forecast model (3) used to determine the free oscillations or normal modes for the initialization procedure is

$$\left.\begin{aligned}\delta_t u&=fv-\frac{g}{a\cos\varphi}\delta_\lambda h\\ \delta_t v&=-fu-\frac{g}{a}\delta_\varphi h\\ \delta_t h&=-\frac{D}{a\cos\varphi}[\delta_\lambda u+\delta_\varphi(v\cos\varphi)]\end{aligned}\right\}, \tag{4}$$

where D is the mean depth corresponding to the equivalent depth of the vertical modes of a baroclinic model.

Following Williamson and Dickinson (1976), the solution of the linearized equations (4) can be written in terms of their free oscillations as

$$\Upsilon(\lambda_i,\varphi_j)=\mathfrak{A}\sum_{k=-M/2}^{M/2}\sum_{m=1}^{L}C(k,m)\mathbf{Y}_j(k,m)\times\exp[i(k\lambda_i+\nu_{km}t)] \tag{5}$$

where M is the number of grid points in the longitudinal direction and L the number of latitudinal modes for each longitudinal wavenumber. Upsilon is the vector of grid point data

$$\Upsilon(\lambda_i,\varphi_j)=\begin{bmatrix}u(\lambda_i,\varphi_j)\\ v(\lambda_i,\varphi_j)\\ h(\lambda_i,\varphi_j)\end{bmatrix}, \tag{6}$$

and $\mathfrak{A}$ a scaling matrix

$$\mathfrak{A}=M^{-\frac{1}{2}}\begin{bmatrix}-i & 0 & 0\\ 0 & 1 & 0\\ 0 & 0 & -i(D/g)^{\frac{1}{2}}\end{bmatrix}. \tag{7}$$

The vector $\mathbf{Y}_j(k,m)$ is the value at latitude φ_j of the mth latitudinal structure function for longitudinal wavenumber k. The frequency of this mode is ν_{km}. The determination of the latitudinal structure functions $\mathbf{Y}$ and their frequencies ν is given in Dickinson and Williamson (1972) and Williamson and Dickinson (1976), hereafter referred to as D&W and W&D, respectively.

The coefficient $c(k,m)$ is the complex amplitude of the (k,m) mode in the expansion of the particular set of grid point data. The method of inverting (5) to determine the coefficients c from a particular set of grid point data at one time is also given in D&W and W&D.

Once the data are expanded into the normal modes, modes which are thought to be erroneous in the data or inconsistent with the forecast model can be eliminated by setting their coefficients to zero.

Before discussing the initialization experiments, we briefly review the nature of the normal modes of the discrete model. A more thorough description is given in D&W. For fixed longitudinal wavenumber k, those modes of the difference equations which correspond closely to the modes of the differential equations are classified as Rossby, eastward or westward gravity modes. These discrete, large-scale modes are given the latitudinal index l of the corresponding continuous modes. The Rossby modes are indexed so that the number of zero crossings increases with increasing l. The $l=0$ Rossby mode is often referred to as the mixed Rossby-gravity wave. The $l=0$ eastward gravity wave takes on the characteristics of Kelvin waves for small equivalent depths. The modes not corresponding to modes of the differential equations are classified as Rossby modes if their frequencies are no larger in magnitude than the frequency of the lowest-index Rossby modes. Likewise, these modes are classified as gravity modes if their frequencies are no smaller in magnitude than the frequency of the lowest-index gravity modes. In general, the frequencies ν of the modes pair up with equal magnitude and opposite sign. One of the pair corresponds to a solution of the continuous equations and is referred to as a "good" mode. The other has a $2\Delta\varphi$ structure modulated by a large-scale wave and is referred to as a "computational" mode. With a 5° grid, these "computational" modes have 18 to 36 zero crossings from pole to pole, but are not necessarily of small scale in the longitudinal direction since they occur with all longitudinal wavenumbers. The distinction between "good" and "computational" Rossby modes is not clear when considering the structure of the smaller latitudinal-scale waves. The high-index "good" modes have a $4\Delta\phi$ scale and, therefore, rather choppy appearance on the discrete grid unlike the corresponding solutions of the continuous equations. Also, their frequencies tend to differ more from the continuous case than do the lower index modes.

3. Initialization experiments

a. Basic experiments

In the first set of experiments presented, we consider a case similar to that of Rasmussen (1974). The shallow water equations are used to forecast the 500 mb heights and winds. The mean depth of the initial data is taken to be that of the 500 mb surface. Such a large mean depth will probably not result in the best possible forecast of the 500 mb height surface, but serves to illustrate the problems expected with a baroclinic model where the external vertical mode has an equivalent depth of around 10^4 m.

The centered-time differences in (3) require initial data at two times, $t=0$ and $t=-\Delta t$. In practice, observed data are generally not available at such small time intervals. Data at these two times have occasionally been taken to be the same for forecasts using the NCAR GCM (Baumhefner, personal communication). When the initial data at the two time levels are the same, we would expect to have some energy in the time-computational modes. These modes, arising from the centered-time finite differences, have a $2\Delta t$ structure and do not correspond to solutions of the continuous equations (see W&D for a discussion of these modes). The expansion method used here [Eq. (5)] does not separate out these time-computational modes given two time levels of data since the expansion depends on only data at one time level. As discussed in W&D, the method does eliminate them if the coefficients $c(k,m)$ are determined at $t=0$ by inverting (5) with $t=0$. Then the data at $-\Delta t$ are obtained from (5) using these coefficients with t set equal to $-\Delta t$.

An indication of the amplitude of the time-computational modes in an integration starting from the same data at $t=0$ and $-\Delta t$ is provided by a plot (Fig. 1a) of the height h at one grid point as a function of time. The initial data for the forecast are the 500 mb height and winds for 1200 GMT 15 January 1958, as analyzed by Baumhefner (1970). The initial data at $t=0$ and $-\Delta t$ are taken to be identical. The figure shows the height at 50°W and 50°N from an integration with $\Delta\varphi=\Delta\lambda=5°$ and $\Delta t=1$ min. The small time step is required for stability because of the convergence of the grid points at the poles; no special smoothing is performed there. The effect of a larger time step with longitudinal Fourier filtering near the poles will be discussed later. The height is plotted every iteration (1440 in one day). The saw-tooth pattern of $2\Delta t$ waves is not seen in the figure since the points are too close together in time. The presence of the $2\Delta t$ waves, or time-computational modes, is seen by the thicker lines in the peaks and troughs—most noticeably between 6 and 14 h. The thickness of the lines indicates the amplitude of the time-computational modes. The amplitude of the $2\Delta t$ waves is less than 2.5 m, whereas the 2–4 h waves have amplitudes up to 100 m. This 2.5 m maximum for the amplitude of the $2\Delta t$ waves holds for all grid points examined in this way.

Fig. 1b shows the plot of the height field at the grid point 50°W, 50°N when data at $t=0$ are obtained from the analyzed height and wind fields as in Fig. 1a, but at $t=-\Delta t$ from the modal expansion (5) with the coefficients determined from the $t=0$ data, then recombined to give grid data with $t=-\Delta t$. This procedure greatly reduces the $2\Delta t$ waves without modifying the waves with lower frequencies. In fact, the 2–4 h waves are virtually the same in both cases. Once the $2\Delta t$ waves are reduced, they do not reappear during the course of the one-day forecast. The $2\Delta t$ waves can also be reduced

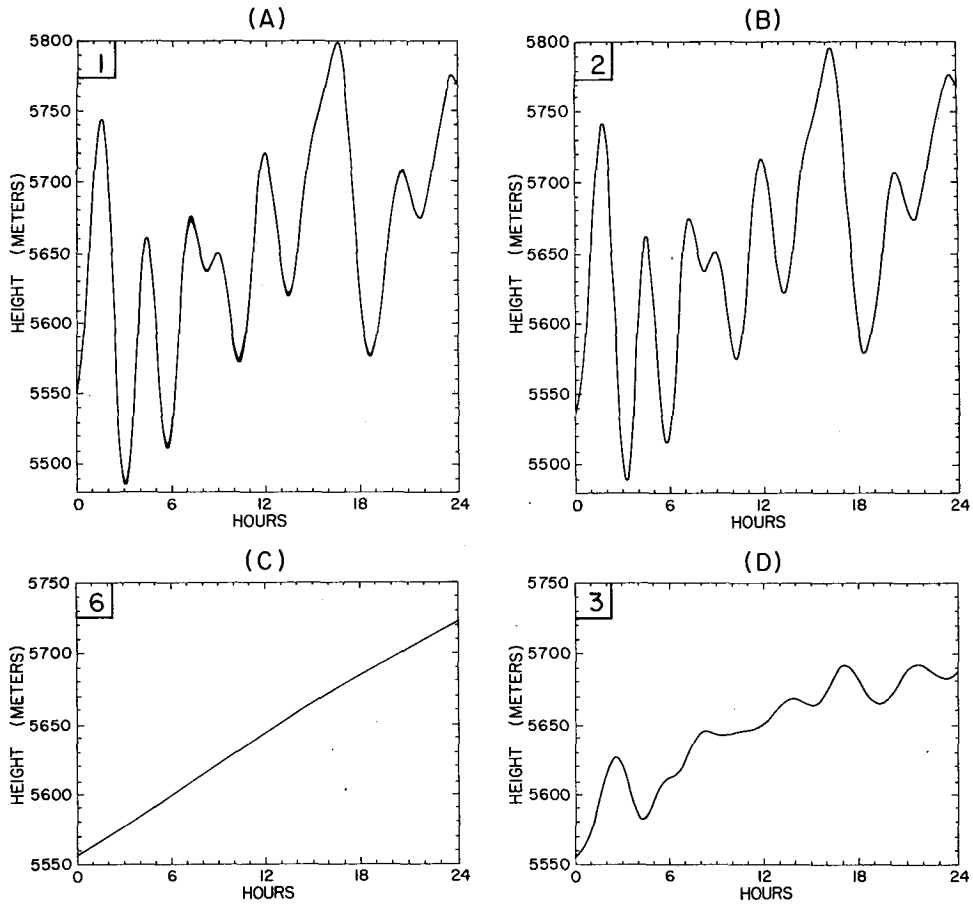

FIG. 1. Height of free surface vs time at grid point 50°W, 50°N for Exps. 1 (a), 2 (b), 6 (c), and 3 (d) of Table 1.

by taking a forward time step initially. In this case, the plot of height as a function of time looks exactly like Fig. 1b.

Note that in both cases starting from analyzed heights and winds (Figs. 1a and 1b), large oscillations appear in the height field with a period of 2–4 h and amplitude up to 100 m. These figures are typical of the oscillations that occur at many grid points in these integrations. Such oscillations are quite similar to those noted by Houghton *et al.* (1971) in forecasts from

TABLE 1. Skill scores of 500 mb height forecasts.

Experiment no.	Description	Northern extratropics 30°N–85°N				Tropics 25°S–25°N				Southern extratropics 85°S–30°S			
		Day 0		Day 1		Day 0		Day 1		Day 0		Day 1	
		S.D. (m)	S_1	S.D. (m)	S_1	S.D. (m)	S_1	S.D. (m)	S_1	S.D. (m)	S_1	S.D. (m)	S_1
1.	Analyzed h & $\mathbf{V}$ at $t=0$ and at $t=-\Delta t$	0	0	88.77	64.6	0	0	52.51	95.9	0	0	76.85	63.2
2.	Analyzed h & $\mathbf{V}$ at $t=0$ and $t=-\Delta t$ from modal expansion	0	0	88.80	64.6	0	0	52.51	95.8	0	0	76.84	63.2
3.	Computational Rossby and all gravity waves removed	37.69	30.9	64.47	43.4	19.73	70.1	28.55	78.3	42.56	36.2	55.73	45.1
4.	Forecast from (2), filtered as (3) after forecast	37.69	30.9	66.23	41.2	19.73	70.1	30.45	80.5	42.56	36.2	55.96	42.9
5.	Linear forecast from initial data of (2)	0	0	132.5	70.2	0	0	53.33	98.1	0	0	96.18	67.6
6.	Linear forecast from initial data of (3)	37.69	30.9	120.0	57.5	19.73	70.1	33.67	86.4	42.56	36.2	80.07	54.8

"balanced" initial data with the NCAR GCM. Such gravity waves can be eliminated from the initial data by means of the modal expansion by simply setting the coefficients of these modes to zero before recombining to get grid point data.

Figs. 1c and 1d show height as a function of time for the same point as discussed above for two integrations in which the amplitudes of the computational Rossby waves and all gravity waves are set to zero. Fig. 1c shows the results of a forecast with the linear equations (4). The gravity waves are eliminated, as they should be and, of course, are not regenerated by the model. Figure 1d shows the results of a forecast with the nonlinear equations (3). We see that some high-frequency waves are generated immediately by the nonlinear interactions; however, their amplitudes are greatly reduced over the cases with no modal filtering. Thus, modal filtering is quite effective in substantially reducing the amplitudes of the high-frequency oscillations in the early periods of numerical forecasts with the shallow water equations.

Although modal filtering does remove the large-amplitude, high-frequency oscillations, it remains to be seen whether or not it improves the forecast at Day 1. We examine this question by considering the standard deviation (S.D.) of the error and the S_1 skill score of the height forecast:

$$\text{S.D.}=\left\{\frac{\sum_{j=J_1}^{J_2}\sum_{i=1}^{I}\left[(h^0_{i,j}-\overline{h^0_{i,j}})-(h^F_{i,j}-\overline{h^F_{i,j}})\right]^2\cos\varphi_j}{I\sum_{j=J_1}^{J_2}\cos\varphi_j}\right\}^{\frac{1}{2}}, \quad (8)$$

$$S_1=100\Big\{\sum_{j=J_1}^{J_2}\sum_{i=1}^{I}\left|(h^F_{i,j}-h^F_{i+1,j})-(h^0_{i,j}-h^0_{i+1,j})\right| + \sum_{j=J_1}^{J_2-1}\sum_{i=1}^{I}\left|(h^F_{i,j}-h^F_{i,j+1})-(h^0_{i,j}-h^0_{i,j+1})\right|\Big\} \div\Big\{\sum_{j=J_1}^{J_2}\sum_{i=1}^{I}\max(|h^F_{i,j}-h^F_{i+1,j}|,\ |h^0_{i,j}-h^0_{i+1,j}|) + \sum_{j=J_1}^{J_2-1}\sum_{i=1}^{I}\max(|h^F_{i,j}-h^F_{i,j+1}|,\ |h^0_{i,j}-h^0_{i,j+1}|)\Big\}, \quad (9)$$

where h^F is the forecast height and h^0 the observed height, I is the number of points in longitude around the earth, J_1 and J_2 are the indices defining the latitude band over which the verification statistics are taken, and the overbar denotes the area-weighted global average. The standard deviation of the error is the same as the rms error of the forecast height field with the mean error removed. The S_1 score is a measure of the normalized height gradient error. Note that smaller values of both skill scores indicate better forecasts.

The shallow water equations (3) should not be considered as a practical forecast model. They lack many physical processes important for atmospheric motions and, as used here, are not tuned to produce the best possible forecast. With this in mind, the skill scores should not be compared with forecasts from other models, but rather should be used to compare various forecasts of the same model starting from different initial data to determine the effect of the various experiments.

Table 1 lists the S.D. of the error and the S_1 scores for the cases discussed above for the latitude bands 30° to 85°, referred to as northern extratropics, −25° to 25° referred to as tropics, and −85° to −30° referred to as southern extratropics. The first two rows present the results from the two cases starting with analyzed heights and winds, the first row with the data at $t=-\Delta t$ equal to that at $t=0$ and the second row with the data at $t=-\Delta t$ determined from the modal expansion. There is virtually no difference between the skill scores of these two cases. The removal of the small $2\Delta t$ waves present in the first forecast has no effect on the skill scores of the one-day forecast. Removal of the gravity waves and computational Rossby waves does improve the forecast, evident from the third row of Table 1. The S.D. is reduced by 20–25 m in all areas and the S_1 score is reduced by 15–20. It is interesting to note the skill scores of the initial data after removing the gravity and computational Rossby waves. In the band from 30° to 85°N, the S.D. is around 37 m and the S_1 score is close to 31. These scores are comparable to the difference between two different analyses. For example, Baumhefner (personal communication) has computed the rms and S_1 scores for the 500 mb height field comparing his subjective analysis with the standard *NMC* analysis for the period 6–14 December 1967. He found that in the latitude band 30°–70°N the rms varies from 27 to 39 m and the S_1 from 29 to 35. The scores for Day 0 in Table 1 fall within this range.

The scores in the tropics after filtering the initial data are quite different from those in the extratropics. The S.D. is lower and the S_1 score is much higher; Fig. 2 gives the reason for this by showing the initial height field before and after filtering. There is little change in the extratropics, except for very slight smoothing. On the other hand, the major features in the tropics, although of small amplitude, are quite different in shape. Thus, the S.D. is low but the reversal of gradients in some areas results in a large S_1 score.

Of course, the question remains as to whether the improved skill scores actually represent a better forecast or are a result of the smoothing due to the initial filtering. Row 4 of Table 1 indicates the latter to be the case. These scores are computed from the second forecast starting from unfiltered data, but the forecast data are filtered before the scores are computed in the same way that initial data for the third case were filtered. Filtering the initial data and then making a forecast

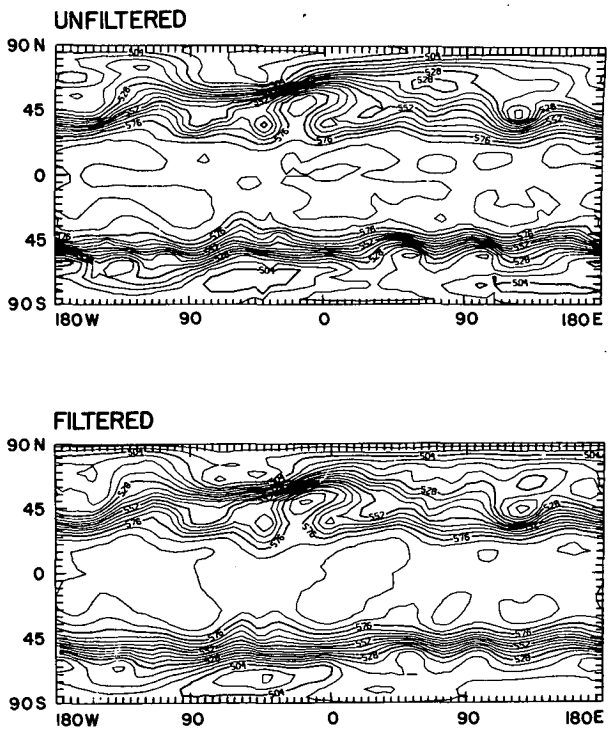

FIG. 2. Initial height field of Exps. 1 (above) and 3 (below) of Table 1. Contour interval is 60 m, contour labels in decameters.

or making a forecast and then filtering the forecast data results in essentially the same skill scores. This implies that the waves removed hardly interact nonlinearly with the Rossby waves during the forecast. Refiltering the third case after the forecast does not change the S.D. by more than 2 m or the S_1 score by more than 2. Thus, the amplitudes of the gravity waves generated during the forecast (seen in Fig. 1) are not great enough to affect the skill scores significantly.

It would also be useful to filter the verification data before computing the skill scores, making it possible to verify certain modes. Unfortunately, since observed winds were not included in Baumhefner's (1970) analysis for 16 January, the verification data cannot be filtered using the normal modes. (Experiments with a different data set containing verification winds and heights are currently underway.)

The last two rows of Table 1 list the skill scores from forecasts made with the linear difference equations (4) starting from filtered and unfiltered data. In both cases, the linear forecasts are inferior to the nonlinear forecasts. This lower skill may be due to the lack of nonlinear interactions or more probably from neglect of a mean wind. The linear model could be improved by adding a mean wind, or by empirically determining the frequency of each mode in atmospheric data and simply using the modal expansion (5) with the frequencies ν_{km} replaced by their empirical values to make a forecast.

b. Elimination of small-scale Rossby waves

We have seen that removing the computational Rossby and all the gravity waves substantially reduces the amplitudes of the high-frequency oscillations during the forecast and improves the skill scores of the one-day forecast. However, there is little reason to expect *a priori* that this particular filter is optimal. Therefore, we have performed additional forecasts to investigate the effect of removing the small-scale, higher-index Rossby waves. Table 2 lists the skill scores for these forecasts with the second and third columns showing the number of modes retained in longitude and latitude.

The longitudinal scale of the smallest mode retained is easily determined. With 36, 18, 12 or 9 modes in longitude, the shortest one has wavelength equal to $2\Delta\lambda$, $4\Delta\lambda$, $6\Delta\lambda$ or $8\Delta\lambda$, respectively, with the 5° grid used for all calculations reported here. The meridional scale of the Rossby modes is not as easily determined since the modes do not have a pure sinusoidal structure in that direction. By determining the zero crossings of the modes in the meridional direction, a latitudinal scale can be associated with the smaller-scale, higher-index modes. When 17 latitudinal modes are retained, i.e., all the good Rossby modes, the scale of the smallest is around $4\Delta\phi$. When 8 latitudinal modes are retained, the scale of the smallest is $5\text{–}6\Delta\phi$ for $k \gtrsim 8$ and increases to $7-8\Delta\phi$ for $k=1$. When 6 latitudinal modes are retained, the scale is $5\text{–}7\Delta\phi$ for the medium longitudinal wavenumbers ($k=8\text{–}12$) and increases to $10\text{–}12\Delta\phi$ for $k=1$. Again, the above scales are for the 5° grid used here.

TABLE 2. Skill scores of 500 mb height forecasts for all gravity waves removed.

Experiment no	Description: Number of Rossby modes in longitude	Description: Number of Rossby modes in latitude	Northern extratropics 30°N–85°N: Day 0 S.D. (m)	Day 0 S_1	Day 1 S.D. (m)	Day 1 S_1	Tropics 25°S–25°N: Day 0 S.D. (m)	Day 0 S_1	Day 1 S.D. (m)	Day 1 S_1	Southern extratropics 85°S–30°S: Day 0 S.D. (m)	Day 0 S_1	Day 1 S.D. (m)	Day 1 S_1
3.	36	17	37.69	30.9	64.47	43.4	19.73	70.1	28.55	78.3	42.56	36.2	55.73	45.1
7.	18	17	37.49	30.1	64.35	42.9	19.71	70.0	28.57	77.8	42.52	35.9	55.52	44.7
8.	18	8	47.59	38.2	74.32	44.9	20.17	72.3	27.85	78.9	50.91	43.2	56.41	42.8
9.	12	6	71.70	46.8	93.45	51.2	21.97	71.8	29.09	79.7	59.08	45.4	61.02	46.0
10.	9	5	96.88	54.5	112.2	58.3	22.27	74.4	28.96	81.0	63.89	48.4	61.09	45.7

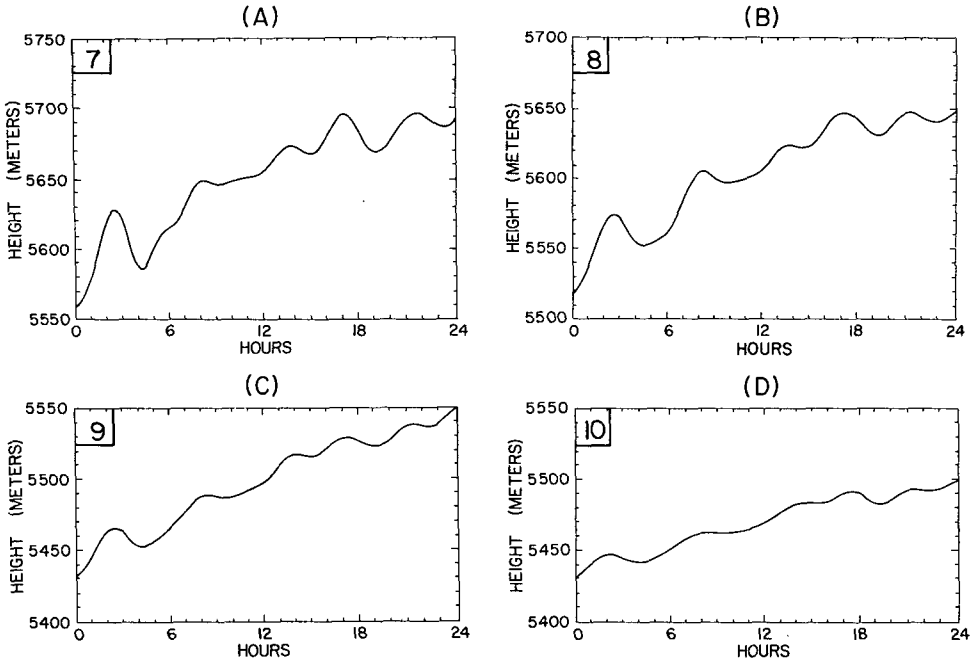

FIG. 3. Height of free surface vs time at grid point 50°W, 50°N for Exps. 7 (a), 8 (b), 9 (c), and 10 (d) of Table 2.

We concentrate first on the skill scores of the one-day forecast of the northern extratropics. Table 2 shows that elimination of half the longitudinal waves (2–4$\Delta\lambda$) has a negligible effect on both skill scores (Exp. 7 vs Exp. 3). Elimination of half the latitudinal waves increases the S.D. while having only a small effect on the S_1 score (Exp. 8 vs Exp. 7). The elimination of additional waves so that only 12 longitudinal and 6 latitudinal waves are retained increases both skill scores. Thus, these waves do provide information in the forecast even though the second-order approximations of the model are less accurate for these waves than for the longer ones (Grammeltvedt, 1969; Kreiss and Oliger, 1973). Since these higher-index modes have lower frequencies, their apparent skill might result from the presence of persistent small-scale features. Further investigation of this question is needed, preferably with cases where the verification data, as well as the forecast and initial data, can be filtered using the normal mode expansion. In the northern extratropics, the skill scores computed by comparing the filtered initial data with the unfiltered initial data show the same pattern as the one-day forecast, i.e., no change when eliminating half the longitudinal waves, an increase in scores when removing half the latitudinal waves, and further increases when removing additional waves.

In the tropics, the elimination of the additional waves listed in Table 2 has little effect on the skill scores of both the initial data and the one-day forecast. In the southern extratropics, the additional filtering is noted in the initial data in the same way as in the northern extratropics, but to a much lesser extent. There is little change in the S_1 score of the one-day forecast, whereas the S.D. of the error increases only slightly with the additional filtering. This minimal effect in the tropics and Southern Hemisphere of the additional filtering is probably due to the lack of detailed structure in the initial and verification data in these areas as seen in Fig. 2.

Figure 3 shows the plots of height as a function of time at the same grid points as in Fig. 1 for the additional forecasts listed in Table 2. Comparison of Fig. 3a with Fig. 1d shows that removal of half the longitudinal Rossby waves (2–4$\Delta\phi$) has no noticeable effect on the height field at this grid point. Comparison of Figs. 3a and 3b shows that removal of half the latitudinal Rossby waves does have an effect, although quite small. The amplitudes and phases of the gravity waves generated during the forecast are quite similar. The height at this point is less after removing the additional waves. Figures 3c and 3d show that removing additional waves again reduces the height at this point and changes the amplitude of the gravity waves generated during the forecast, although the phases are similar in all cases.

c. *Addition of large-scale gravity waves*

In previous experiments, all gravity waves were removed. However, the lower-index, large-scale gravity modes may not be detrimental to the forecast and in some cases may be vital to obtain the correct solution. Therefore, we have performed another series of experiments adding some of the low-order gravity waves to the initial data of the best case in Table 2, i.e., that in which the 2–4$\Delta\lambda$ Rossby waves are removed as well as

TABLE 3. Skill scores of 500 mb height forecasts with 18 longitude and 17 latitude Rossby waves retained.

Experiment no.	Number of gravity modes in longitude	Number of gravity modes in latitude	Northern extratropics 30°N–85°N Day 0 S.D. (m)	S_1	Day 1 S.D. (m)	S_1	Tropics 25°S–25°N Day 0 S.D. (m)	S_1	Day 1 S.D. (m)	S_1	Southern extratropics 85°S–30°S Day 0 S.D. (m)	S_1	Day 1 S.D. (m)	S_1
7.	0	0	37.49	30.1	64.35	42.9	19.71	70.0	28.57	77.8	42.52	35.9	55.52	44.7
11.	9	1	36.23	29.9	65.82	43.5	17.13	68.8	32.86	79.6	42.73	35.8	55.24	44.2
12.	9	2	32.10	29.9	65.63	43.6	17.80	68.0	39.22	81.3	40.34	35.1	59.66	44.7
13.	9	5	28.63	29.3	74.38	44.1	14.03	64.8	39.65	83.9	35.66	33.4	66.67	46.0
14.	18	17	28.75	37.7	81.73	54.2	9.57	53.0	47.91	94.1	29.96	42.5	73.94	54.4

the computational Rossby waves (Exp. 7). The skill scores from these experiments are listed in Table 3. In the first additional experiment (Exp. 11), we include the first latitudinal gravity mode for the first 9 longitudinal modes. There is essentially no change in the extratropical skill scores and a very small increase in the tropical skill scores of the one-day forecast. The addition of one more latitudinal gravity mode for the first 9 longitudinal modes (Exp. 12) again does not affect the northern extratropics, but does increase the skill scores in the tropics, being not much less than the skill scores when 9 longitudinal and 5 latitudinal gravity waves are included. This case (Exp. 13) increases the extratropical skill scores, but not to the extent of including 18 longitudinal and 17 latitudinal gravity modes (Exp. 14). Even in this case (Exp. 14), the skill scores are not as large as when all Rossby and gravity modes are included (Exp. 1).

Figure 4 shows the grid point plots from the experiments set forth in Table 3 in which low-order gravity waves are included. Comparing Figs. 4a and 3a shows no effect of adding the first latitudinal gravity mode for the first 9 longitudinal modes. Comparing 4b and 4a shows no effect of adding the second latitudinal mode during the first 12 h of the forecast; the second 12 h show a different evolution, with no significant change

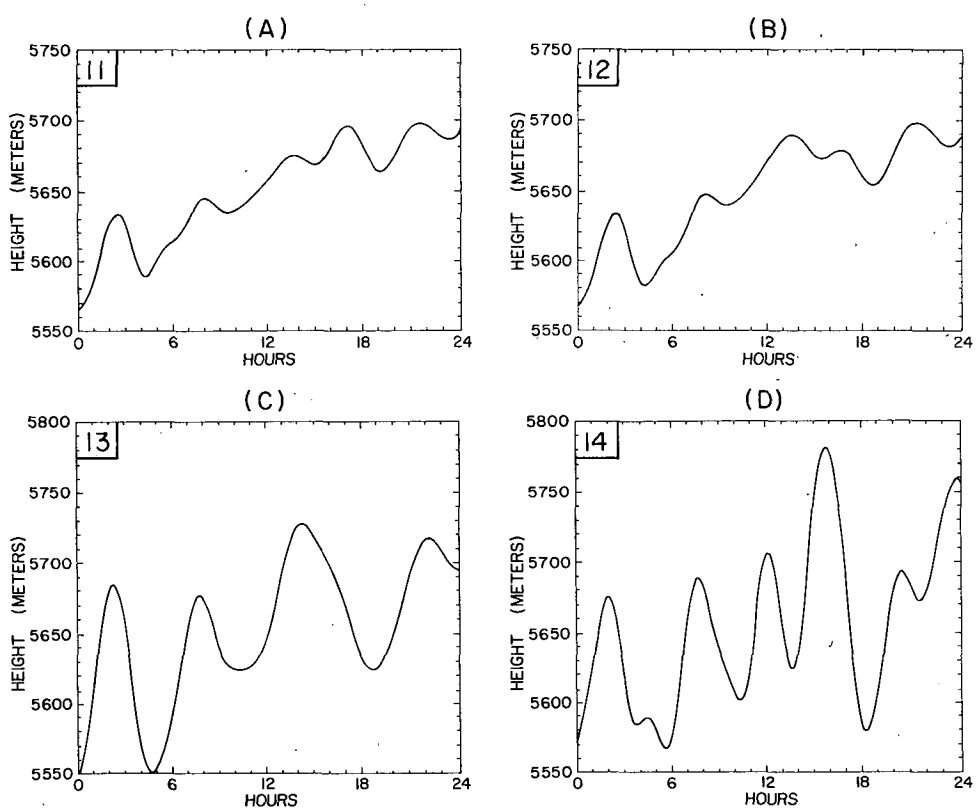

FIG. 4. Height of free surface vs time at grid point 50°W, 50°N for Exps. 11 (a), 12 (b), 13 (c), and 14 (d) of Table 3.

TABLE 4. Skill scores of 500 mb height forecasts with mean depth reduced to 1500 m.

Experiment no.	Description	Northern extratropics 30°N–85°N Day 0 S.D. (m)	S_1	Day 1 S.D. (m)	S_1	Tropics 25°S–25°N Day 0 S.D. (m)	S_1	Day 1 S.D. (m)	S_1	Southern extratropics 85°S–30°S Day 0 S.D. (m)	S_1	Day 1 S.D. (m)	S_1
15.	Analyzed h & **V** at $t=0$ and $t=-\Delta t$ from modal expansion	0	0	64.86	52.4	0	0	32.24	84.7	0	0	53.96	51.7
16.	Computational Rossby and all gravity modes removed	27.87	27.8	58.18	41.3	17.37	68.6	24.21	79.0	32.36	32.5	48.17	43.8
17.	All gravity waves removed, 18 longitude and 17 latitude Rossby waves retained	27.69	27.1	57.98	40.8	17.37	68.6	24.20	78.7	32.39	32.4	48.00	43.5
18.	All gravity waves removed, 18 longitude and 8 latitude Rossby waves retained	42.56	37.5	69.46	43.5	18.20	72.0	24.34	79.2	45.09	41.9	51.69	43.8
19.	18 longitude and 17 latitude Rossby waves retained, 9 longitude and 5 latitude gravity waves retained	23.90	26.6	60.30	41.4	13.73	67.9	26.85	77.4	29.30	31.2	49.37	43.5

in overall amplitude. Inclusion of 9 longitudinal and 5 latitudinal modes (Fig. 4c) results in much larger amplitudes of the high-frequency waves, and inclusion of 18 longitudinal and 17 latitudinal modes (Fig. 4d) shows even larger amplitudes along with higher frequencies.

d. Forecasts with smaller mean depth

The previous forecasts were carried out using the mean depth of the 500 mb surface for the initial data. In this case, the gravity modes have frequencies close to the external modes of a baroclinic forecast model. As the mean depth decreases, the frequency of each mode decreases. Smaller mean depths correspond to internal vertical modes of a baroclinic mode. We repeated several previous experiments with the mean depth of the data decreased to 1500 m to test its effect on the modal filtering. Several investigators (Puri and Bourke, 1974; Daley, 1974) have used this value of the mean height to slow down the waves and improve the forecast of the shallow water equations. Table 4 lists the skill scores for the experiments using 1500 m for the mean depth. The initial data for Exp. 15 are the analyzed heights and winds at $t=0$ with the mean height changed to 1500 m. The data for $t=-\Delta t$ were obtained by expanding the data at $t=0$ into the normal modes for a linear model with mean depth of 1500 m and reevaluating it at the grid points at $t=-\Delta t$. Comparison of the skill scores from this experiment with those of Exp. 2 in Table 1, where the mean depth was that of the 500 mb height field, shows that the decreased mean depth produces a more accurate forecast by slowing down the waves. Experiment 16 in Table 4 uses initial data from which the computational Rossby waves and all gravity waves are removed. As in the experiments using the larger mean depth, the verification scores are improved by the filtering, although not as dramatically with the smaller mean depth. With the mean depth of 1500 m, the S_1 score shows a larger decrease from filtering than the S.D. in the extratropics.

The additional removal of the $2\text{–}4\Delta\lambda$ Rossby modes (Exp. 17) hardly affects the forecast. The removal of half the latitudinal Rossby modes (Exp. 18) decreases the quality of the forecast in the extratropics, especially the S.D. in the Northern Hemisphere. These results are essentially in agreement with the earlier forecasts using the larger mean depth. The last forecast in Table 4 includes 18 longitudinal and 17 latitudinal Rossby waves and 9 longitudinal and 5 latitudinal gravity waves. This filtering is the same as Exp. 13 of Table 3. The degradation of the forecast by the addition of these gravity waves is much less when using smaller mean depth (1500 m) than with the observed 500 mb mean depth. Since the atmosphere contains a stationary component which is not approximated well by the shallow water equations, the degradation due to the additional gravity waves may be less with the smaller mean depth because the frequencies of the modes are smaller in this case.

Figure 5 shows the plots of height as a function of time for the forecasts listed in Table 4 at the same grid point as the previous figures. Note that the height is less in this figure than in the previous ones since the mean depth is decreased but the scale is the same. Figure 5a is the forecast from initial data with no modal filtering. Comparison with Fig. 1b shows that the amplitudes of the oscillations are somewhat less than those for the larger mean depth, although still not negligible. Figure 5b gives the results of removing the computational Rossby waves and all gravity waves from the initial data. The corresponding case with the larger equivalent depth is shown in Fig. 1d. Comparison of the two shows that the amplitudes of the higher-frequency waves are similar in the two cases and the frequencies

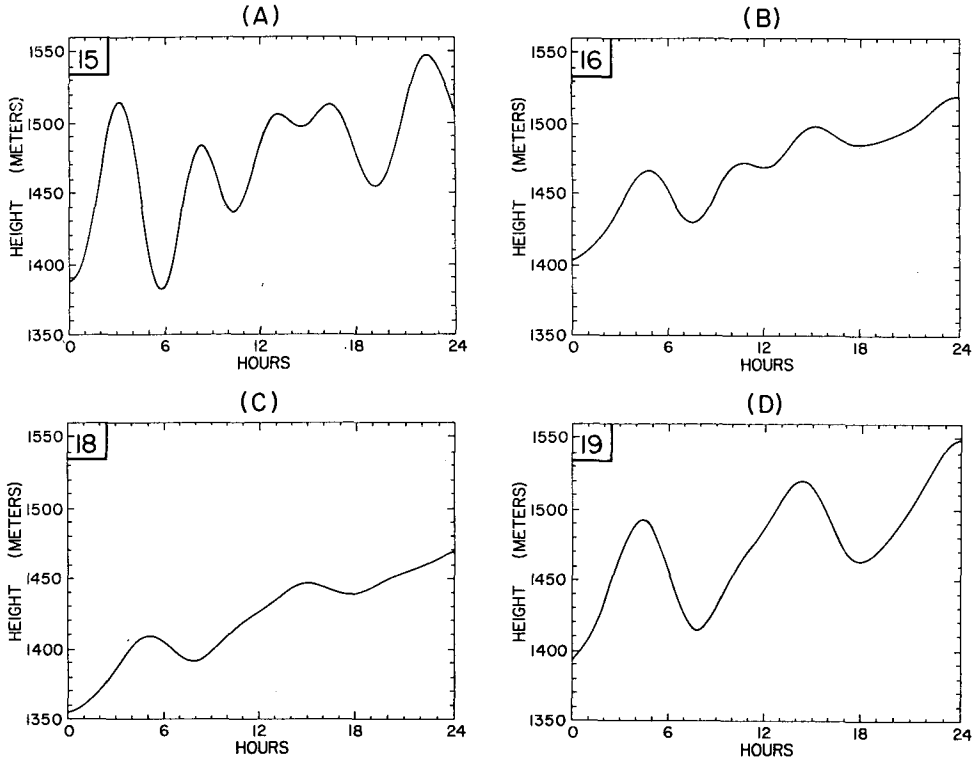

FIG. 5. Height of free surface vs time at grid point 50°W, 50°N for Exps. 15 (a), 16 (b), 18 (c), and 19 (d) of Table 4. In these forecasts, the mean height was reduced to 1500 m.

are somewhat less with the smaller equivalent depth. This latter feature is expected since the frequency of each mode is less for the smaller equivalent depth.

Additional removal of the $2\text{–}4\Delta\lambda$ Rossby waves (Exp. 17) does not affect the subsequent evolution of the height field at this particular grid point. The plot from Exp. 17 is identical to that of Exp. 16 (Fig. 1b) and thus is not included. The additional removal of half the latitudinal Rossby waves (Exp. 18, Fig. 5c) reduces the amplitude of the high-frequency oscillations slightly, although the effect is small. The addition of the large-scale gravity waves (Exp. 19, Fig. 5d) increases the amplitude of the noise in the forecast, although the amplitude is not as large as with the unfiltered data (Fig. 5a).

e. Effect of polar filtering

All of the previous experiments have been performed using a grid uniform in latitude and longitude which requires a relatively small time step for computational stability. Such a system would not be used in an operational situation. Holloway *et al.* (1973) and Williamson and Browning (1973) have shown that the time step can be increased by Fourier filtering the prognostic variables near the poles in the longitudinal direction to eliminate the short-wavelength, high-frequency waves. Williamson (1976) examined the effect of this filtering on the normal modes of the system and determined the corresponding linear stability condition.

We repeated several previous experiments using polar filtering and a longer time step. We used a 6 min time step for the cases with the mean depth of the 500 mb surface filtering at latitudes down to 65°, as in Williamson and Browning (1973), and filtering only at 85°, as in Williamson (1976). In no cases were there significant differences in the skill scores with and without this polar filtering. In the tropics, the scores agreed to 4 digits, whereas in the extratropics they agreed to at least 2 digits. The grid point plots were also essentially the same except for a slightly larger $2\Delta t$ component and a slight change near the poles. The $2\Delta t$ component was still extremely small. The differences near the poles were noticeable only in the highest frequencies and the basic structure in the plots was the same. The same agreement was seen in forecasts using 1500 m mean depth and a 6 or 12 min time step with polar filtering.

4. Conclusions

We tested with the shallow water equations the method proposed by Dickinson and Williamson (1972) to initialize data for a forecast model by expanding the data into the free oscillations or normal modes of the particular model. These modes are classified as Rossby waves, eastward and westward gravity waves, and computational modes according to their correspondence with the modes of the tidal equations. The forecast model consists of the shallow water equations with second-order centered difference approximations over a

uniform latitude-longitude global grid. The normal modes were determined from the linearized version of the forecast model.

The model was used to forecast the 500 mb heights and winds from observed data for 1200 GMT 15 January 1958. The mean depth for most of the experiments was that of the observed 500 mb surface. Such a large mean depth does not produce the best possible forecast with the shallow water equations, but serves to illustrate the problems expected with a baroclinic model where the external vertical mode has an equivalent depth of around 10^4 m.

In the forecasts starting from analyzed heights and winds with no modal filtering, large oscillations appear in the height field with a period of 2–4 h and amplitudes as large as 100 m. These oscillations are typical of the large-amplitude, high-frequency oscillations found in the early stages of forecasts with many primitive equation models starting with either observed or "balanced" data.

These oscillations are eliminated when the normal mode initialization procedure is used to remove the computational Rossby waves and all the gravity waves from the initial data. The standard deviation of the error and the S_1 skill score show substantial improvement in the filtered case in all regions considered. The improved skill scores are a result of smoothing due to the initial filtering rather than a better forecast of the modes retained. The same improvement in the skill scores is obtained by filtering the forecast data after the forecast is made from unfiltered data and then computing the skill scores. Thus, the waves removed from the initial data do not interact significantly with the Rossby waves during the one-day forecast with the shallow-water equations. This may not be the case with more complicated forecast models which include moisture processes.

The particular filtering used in the above forecasts is not necessarily the most suitable. The larger-scale gravity waves with their associated divergence may provide useful information in the forecast while the smaller-scale Rossby waves may not because they are approximated poorly by the finite differences or poorly represented in the data. Additional forecasts were performed to examine the effect of the removal of the smaller-scale Rossby modes. Removal of half the longitudinal Rossby modes (2–$4\Delta\lambda$) does not affect the skill scores. Removal of half the latitudinal Rossby modes increases the skill scores in the northern extratropics, indicating that these modes do provide some information in the forecast. Removal of these modes has little effect in the tropics and southern extratropics where the initial and verification data of this case are relatively smooth. Removal of additional Rossby modes degrades the forecasts even more in both the northern and southern extratropics, but to a lesser extent in the southern extratropics.

A third set of forecasts was performed to examine the effect of the large-scale gravity waves on the forecasts. In essence, the largest-scale gravity waves have little effect on the skill scores of the forecasts. The scores in the extratropics are the same with or without the extra gravity waves, while there is a small increase in tropical scores indicating a poorer forecast there when the waves are included. The addition of higher-index gravity waves degrades the skill scores in all regions. The importance of the largest-scale gravity waves must be examined more thoroughly in forecasts with baroclinic models.

A few experiments were repeated changing the mean depth of the initial data to 1500 m to test the effect of slower phase speeds on the initialization procedure. The smaller mean height is often used to slow down the waves in the barotropic model. The normal modes used for these experiments were those for a shallow water model with a mean depth of 1500 m, which have lower frequencies and somewhat different shapes from those with a mean depth of the 500 mb surface. When the same filtering is performed, the smaller equivalent depth results in a better forecast in terms of the skill scores. In comparing the results of different initial filtering on the forecasts using 1500 m depth, there are no differences from the conclusions found in the forecasts using the actual 500 mb heights, although the impact of the filtering is less dramatic with the 1500 m depth.

Several forecasts were repeated using longitudinal fourier filtering near the poles to allow a longer stable time step. The modes corresponding to the actual filtering were used for the initialization. In no cases were there significant differences in the skill scores with the various polar filters.

The modal initialization scheme has been derived and coded for the multi-level NCAR global circulation model. The modal scheme will be compared with other initialization procedures and with the use of a time filter in forecasts with this model.

Acknowledgments. I thank David Baumhefner for providing the initial and verification data and for allowing me to publish his unpublished skill scores computed by comparing two different analyses. I also thank Robert Dickinson and Akira Kasahara for many helpful comments on the manuscript, Gerald Browning for programming assistance, and Ann Lundberg for editorial assistance and typing.

REFERENCES

Baumhefner, D. P., 1970: Global real-data forecasts with the NCAR two-level general circulation model. *Mon. Wea. Rev.*, **98**, 92–99.

Bourke, W., 1974: A multi-level spectral model. I. Formulation and hemispheric integrations. *Mon. Wea. Rev.*, **102**, 687–701.

Charney, J., 1955: The use of the primitive equations of motion in numerical prediction. *Tellus*, **7**, 22–26.

Daley, R., 1974: Cross-equatorial error propagation: A numerical simulation. *Atmosphere*, **12**, 125–132.

Dickinson, R. E., and D. L. Williamson, 1972: Free oscillations of a discrete stratified fluid with application to numerical weather prediction. *J. Atmos. Sci.*, **29**, 623–640.

Grammeltvedt, A., 1969: A survey of finite-difference schemes for the primitive equations for a barotropic fluid. *Mon. Wea. Rev.*, **97**, 384–404.

Hinkelmann, K., 1951: Der Mechanismus des meteorologischen Lärmes. *Tellus*, **3**, 285–296.

Holloway, J. L., Jr., M. J. Spelman and S. Manabe, 1973: Latitude-longitude grid suitable for numerical time integration of a global atmospheric model. *Mon. Wea. Rev.*, **101**, 69–78.

Houghton, D., and W. Washington, 1969: On global initialization of the primitive equations: Part 1. *J. Appl. Meteor.*, **8**, 726–737.

——, D. P. Baumhefner and W. M. Washington, 1971: On global initialization of the primitive equations: Part II. The divergent component of the horizontal wind. *J. Appl. Meteor.*, **10**, 626–634.

Kreiss, H., and J. Oliger, 1973: Methods for the approximate solution of time dependent problems. *GARP Publ. Ser.* No. 18, 107 pp.

Phillips, N. A., 1963: Geostrophic motions. *Rev. Geophys.*, **1**, 123–176.

Puri, K., and W. Bourke, 1974: Implications of horizontal resolution in spectral model integrations. *Mon. Wea. Rev.*, **102**, 333–347.

Rasmussen, E., 1974: An investigation of the truncation errors in a barotropic primitive equations model on spectral form. Rept. No. 5, Institute for Theoretical Meteorology, University of Copenhagen, Denmark, 40 pp.

Washington, W. M., and D. P. Baumhefner, 1975: A method of removing Lamb waves from initial data for primitive equation models. *J. Appl. Meteor.*, **13**, 114–119.

Williamson, D. L., 1976: Linear stability of finite-difference approximations on a uniform latitude-longitude grid with fourier filtering. *Mon. Wea. Rev.*, **104** (to appear).

——, and G. L. Browning, 1973: Comparison of grids and difference approximations for numerical weather prediction over a sphere. *J. Appl. Meteor.*, **12**, 264–274.

——, and R. E. Dickinson, 1976: Free oscillations of the NCAR global circulation model. (In preparation.)